Electronic Supplementary Information (ESI)

Tetraphenylethylene or Naphthalimide-Functionalized Dendritic Carbazole AIEgens: Self-Assembly Visualization, Three Disparate Force-Triggered Fluorescence Responses, and Advanced Anticounterfeiting Applications

Yijie Zou,[a] Zhao Chen,*[a] Fei Zhao,[a] Ya Yin,[d] Kaixin He,[a] Xingru Liang,[a] Hai-feng He,*[c] Zhijian Li,*[a] and Sheng Hua Liu*[b]

[a] Jiangxi Province Key Laboratory of Organic Functional Molecules; Institute of Organic Chemistry, Jiangxi Science and Technology Normal University, Nanchang 330013, PR China

[b] State Key Laboratory of Green Pesticide, College of Chemistry, Central China Normal University, Wuhan 430079, PR China

[c] School of Chemistry and Chemical Engineering, Jiangxi Science and Technology Normal University, Nanchang 330013, PR China

[d] State Key Laboratory of Coordination Chemistry, School of Chemistry and Chemical Engineering, Nanjing University, Nanjing 210023, PR China

*Corresponding Author(s): 1020160936@jxstnu.edu.cn; hehf0427@jxstnu.com.cn; lizhijianhdd@163.com; chshliu@mail.ccnu.edu.cn

Contents

1. Experimental Section

Materials and methods

All synthetic experiments were carried out under an argon atmosphere applying standard Schlenk techniques, unless otherwise noted. The reactive materials *N*-(4-iodophenyl)acetamide, (2-(4-bromophenyl)ethene-1,1,2-triyl)tribenzene, 6-bromo-2-hexyl-3a,4-dihydro-1*H*-benzo[*de*]isoquinoline-1,3(2*H*)-dione, $Pd_2(dba)_3$, *t*-BuONa, $P(t\text{-}Bu)_3$ were purchased directly from commercial companies (J&K Chemical Ltd., Innochem and Alfa aesar). All the other starting substances and all reagents were commercially available and used without further purification. The intermediates **I**, **II**, and **III** were synthesized according to the corresponding literature.[1] The expected solid products were acquired from relevant intermediates by substitution reactions.[2] Thin-layer chromatography analysis was performed using pre-coated glass plates. Silica gel (200-300 mesh) was used for column chromatography. All nuclear magnetic resonance (NMR) tests were measured on Bruker AVANCE NEO 500 MHz FT-NMR Spectrometer [$CDCl_3$ as a solvent and tetramethylsilane (TMS) as the internal standard]. ^1H NMR spectra were reported as followed: chemical shift in ppm (δ) relative to the chemical shift of TMS at 0.00 ppm, integration, multiplicities (s = singlet, d = doublet, t = triplet, m = multiplet), and coupling constant (Hz). ^{13}C NMR chemical shifts reported in ppm (δ) relative to the central line of triplet for $CDCl_3$ at 77 ppm. High-Resolution Mass Spectrometer (HRMS) spectra were recorded by Bruker AmaZon SL Ion Trap Mass spectrometer. The Agilent 8453 ultraviolet-visible (UV-vis) spectrophotometer was used to measure UV-vis absorption spectra.

Photoluminescence spectra were measured by a Hitachi-F-4600 fluorescence spectrophotometer or a photoluminescence (PL) spectrometer FLS1000 (Edinburgh Instruments). The aggregate behaviors of six carbazole AIEgens in DMF/water mixture (water content: 90%) and the poor solvent-induced self-assembly property of **3CzB2Nap** were investigated by scanning electron microscopy (SEM, Zeiss, Sigma). The X-ray crystal-structure determination of carbazole derivative **3CzB2TPE** was performed on a Bruker APEX DUO CCD system, and the corresponding crystallographic data of **3CzB2TPE** have been deposited in the Cambridge Crystallographic Data Centre as supplemental publication CCDC 2419146. The powder X-ray diffraction (XRD) data were recorded on a Shimadzu XRD-6000 diffractometer using Ni-filtered and graphite-monochromated Cu Kα radiation (λ = 1.54 Å, 40 kV, 30 mA). Fluorescence lifetimes and the absolute fluorescence quantum yields were recorded on Edinburgh Instruments FLS1000 spectrophotometer. DSC data were recorded on Simultaneous Thermal Analyzer (Mettler Toledo, DSC1 Star System). Density functional theory calculations were carried out using Gaussian 16 programs throughout this article. The optimizations of positions of H atoms in single-crystal XRD data were performed using B3LYP hybrid functional[3] with Grimme's dispersion correction of D3 version (Becke-Johnson damping)[4]. The standard 6-31G* basis set[5,6] for all atoms was used. It is said that the reasonable HOMO- LUMO gaps can be obtained at this theoretical level.[7] The isosurfaces of canonical molecular orbitals are obtained by Multiwfn[8] and VMD[9] program.

Synthesis of carbazole derivatives **1CzB2TPE**, **3CzB2TPE** and **7CzB2TPE**:

compounds were synthesized in a similar manner. Taking the synthetic procedure of **1CzB2TPE** as a representative example. The mixture of **1** (1234.0 mg, 3.0 mmol), Pd2(dba)$_3$ (57.4 mg, 0.1 mmol), *t*-BuONa (384.4 mg, 4.0 mmol) in toluene (60 mL), and the corresponding intermediate compound **I** (258.3 mg, 1.0 mmol) in toluene (80 mL) were refluxed with stirring for 48 hours. After the mixture was cooled to room temperature, the crude product was poured into water and filtrated out by dichloromethane, organic layer was washed by brine and dried sodium sulfate. The objective solid was gained by silica gel column chromatography.

1CzB2TPE: yellow-green solid, yield: 71%. ^{1}H NMR (500 MHz, CDCl$_3$): δ (ppm) = 8.07 (d, *J* = 12.5 Hz, 2H), 7.34 (t, *J* = 2.5 Hz, 4H), 7.28 (d, *J* = 8.5 Hz, 2H), 7.22-7.20 (m, 2H), 7.09-6.99 (m, 28H), 6.97-6.95 (m, 4H), 6.86 (d, *J* = 8.5 Hz, 4H), 6.80 (d, *J* = 8.0 Hz, 4H). ^{13}C NMR (125 MHz, CDCl$_3$): δ (ppm) = 145.3, 144.0, 143.7, 143.5, 141.0, 140.7, 140.5, 138.7, 132.3, 131.4, 127.7, 127.6, 127.6, 126.5, 126.4, 126.4, 125.8, 124.2, 123.4, 123.2, 120.2, 119.7, 109.8. HRMS-ESI (m/z): Found: [M + H]$^+$ 919.4054; “molecular formula $C_{70}H_{50}N_2$” requires [M + H]$^+$ 919.4047.

3CzB2TPE: faint green solid, yield: 66%. ^{1}H NMR (500 MHz, CDCl$_3$): δ (ppm) = 8.19 (d, *J* = 1.5 Hz, 2H), 8.09 (d, *J* = 7.5 Hz, 4H), 7.59 (d, *J* = 8.5 Hz, 2H), 7.55-7.53 (m, 2H), 7.45-7.42 (m, 2H), 7.35-7.31 (m, 8H), 7.23-7.20 (m, 4H), 7.16 (d, *J* = 2.5 Hz, 2H), 7.09-7.00 (m, 26H), 7.98-7.96 (m, 4H), 6.90-6.88 (m, 4H), 6.84 (t, *J* = 4.5 Hz, 4H). ^{13}C NMR (125 MHz, CDCl$_3$): δ (ppm) = 147.4, 145.2, 144.0, 143.6, 143.5, 142.8, 140.9, 140.5, 139.0, 132.4, 131.4, 131.4, 131.3, 130.1, 127.7, 127.6, 127.6, 126.5, 126.4, 125.9, 123.7, 123.1, 120.3, 119.7,111.38, 109.7. HRMS-ESI (m/z): Found: [M + H]$^+$ 1250.5251; "molecular formula $C_{94}H_{64}N_4$" requires [M + H]$^+$ 1250.5238.

7CzB2TPE: faint green solid, yield: 62%. ^{1}H NMR (500 MHz, $CDCl_3$): δ (ppm) = 8.45 (d, *J* = 2.0 Hz, 2H), 8.24 (d, *J* = 2.0 Hz, 4H), 8.09 (d, *J* = 8.0 Hz, 8H), 7.75 (t, *J* = 5.3 Hz, 2H), 7.60 (d, *J* = 8.5 Hz, 4H), 7.55-7.53 (m, 4H), 7.33 (t, *J* = 3.8 Hz, 16H), 7.22-7.19 (m, 10H), 7.08-7.01 (m, 30H), 6.98-6.96 (m, 4H), 6.92 (d, *J* = 9.0 Hz, 4H), 6.87 (d, *J* = 8.5 Hz, 4H). ^{13}C NMR (125 MHz, $CDCl_3$): δ (ppm) = 147.7, 145.1, 144.0, 143.6, 143.5, 141.8, 141.6, 141.5, 141.0, 140.4, 139.2, 132.4, 131.4, 131.4, 131.3, 130.2, 127.7, 127.7, 127.6, 126.6, 126.5, 126.4, 126.3, 125.9, 123.8, 123.8, 123.1, 120.3, 119.9, 119.8, 119.7, 111.9, 111.2, 109.7, 29.7. HRMS-ESI (m/z): Found: [M + H]$^+$ 1910.6461; "molecular formula $C_{142}H_{92}N_8$" requires [M + H]$^+$ 1910.7552.

Synthesis of carbazole derivatives **1CzB2Nap**, **3CzB2Nap** and **7CzB2Nap**: compounds were synthesized in a similar manner. Taking the synthetic procedure of **1CzB2Nap** as a representative example. To a solution of **2** (1086.8 mg, 3.0 mmol), $Pd_2(dba)_3$ (57.4 mg, 0.1 mmol), *t*-BuONa (384.4 mg, 4.0 mmol) in toluene (60 mL) was added corresponding intermediate compound **I** (258.3 mg, 1.0 mmol) and toluene solution of P(*t*-Bu)$_3$ (2 mL), and refluxed for 48 hours. After cooling to room temperature, the mixture was poured into water and extracted with CH_2Cl_2. The collected organic layer was washed with brine, dried over anhydrous Na_2SO_4, and concentrated in vacuum. In the end, the pure product was obtained by purification with silica gel column chromatography.

1CzB2Nap: orange solid, yield: 68%. ^{1}H NMR (500 MHz, $CDCl_3$): δ (ppm) =

8.63 (d, *J* = 7.5 Hz, 2H), 8.55 (d, *J* = 7.5 Hz, 2H), 8.29 (d, *J* = 8.5 Hz, 2H), 8.14 (d, *J* = 8.0 Hz, 2H), 7.63 (t, *J* = 7.8 Hz, 2H), 7.50 (d, *J* = 8.0 Hz, 2H), 7.42 (d, *J* = 7.5 Hz, 6H), 7.30 (t, *J* = 6.8 Hz, 2H), 7.16 (d, *J* = 8.0 Hz, 2H), 4.18 (t, *J* = 7.3 Hz, 4H), 1.74 (t, *J* = 7.0 Hz, 4H), 1.44 (s, 4H), 1.35 (s, 8H), 0.90 (d, *J* = 6.5 Hz, 6H). ^{13}C NMR (125 MHz, $CDCl_3$): δ (ppm) = 164.0, 163.4, 131.9, 131.7, 128.4, 127.4, 126.0, 125.0, 124.6, 123.4, 120.4, 120.2, 109.5, 40.5, 31.5, 28.1, 26.8, 22.6, 14.1. HRMS-ESI (m/z): Found: $[M + H]^+$ 817.3744; "molecular formula $C_{54}H_{48}N_4O_4$" requires $[M + H]^+$ 817.3749.

3CzB2Nap: orange solid, yield: 65%. ^{1}H NMR (500 MHz, $CDCl_3$): δ (ppm) = 8.65 (d, *J* = 7.0 Hz, 2H), 8.58 (d, *J* = 7.5 Hz, 2H), 8.34 (d, *J* = 8.5 Hz, 2H), 8.28 (s, 2H), 8.16 (d, *J* = 7.5 Hz, 4H), 7.69-7.63 (m, 8H), 7.49 (d, *J* = 7.5 Hz, 2H), 7.41-7.37 (m, 8H), 7.29 (d, *J* = 7.0 Hz, 4H), 7.24 (s, 2H), 4.19 (t, *J* = 7.0 Hz, 4H), 1.76-1.72 (m, 4H), 1.45 (s, 4H), 1.35 (s, 8H), 0.91, (d, *J* = 6.5 Hz, 6H). ^{13}C NMR (125 MHz, $CDCl_3$): δ (ppm) = 163.9, 163.4, 149.8, 141.7, 140.4, 131.9, 130.6, 127.5, 126.3, 125.9, 125.2, 124.0, 123.2, 120.4, 120.3, 119.8, 119.8, 111.1, 109.6, 40.6, 31.5, 28.1, 26.8, 22.6, 14.1. HRMS-ESI (m/z): Found: $[M + H]^+$ 1147.4906; "molecular formula $C_{78}H_{62}N_6O_4$" requires $[M + H]^+$ 1147.4906.

7CzB2Nap: orange solid, yield: 60%. ^{1}H NMR (500 MHz, $CDCl_3$): δ (ppm) = 8.67 (d, *J* = 7.0 Hz, 2H), 8.58 (t, *J* = 17.3 Hz, 4H), 8.37 (d, *J* = 8.5 Hz, 2H), 8.30 (d, *J* = 13.5 Hz, 4H), 8.16 (d, *J* = 7.0 Hz, 8H), 7.86 (d, *J* = 7.5 Hz, 2H), 7.80 (d, *J* = 8.5 Hz, 2H), 7.73-7.60 (m, 12H), 7.52 (d, *J* = 8.0 Hz, 2H), 7.39 (s, 18H), 7.29 (t, *J* = 13.0 Hz, 8H), 4.20 (t, *J* = 7.0 Hz, 4H), 1.75 (t, *J* = 6.3 Hz, 4H), 1.44 (d, *J* = 6.0 Hz, 4H), 1.35 (s, 8H), 0.91 (d, *J* = 6.5 Hz, 6H). ^{13}C NMR (125 MHz, $CDCl_3$): δ (ppm) = 163.9, 163.4, 149.7, 141.8, 141.5, 141.0, 130.1, 126.3, 125.9, 123.9, 123.8, 123.1, 120.6, 120.3, 119.9, 119.7, 111.1, 109.6, 40.6, 31.5, 28.1, 26.8, 22.6, 14.1. HRMS-ESI (m/z): Found: $[M + H]^+$ 1808.7250; "molecular formula $C_{126}H_{90}N_{10}O_4$" requires $[M + H]^+$ 1808.7253.

2. Scheme S1

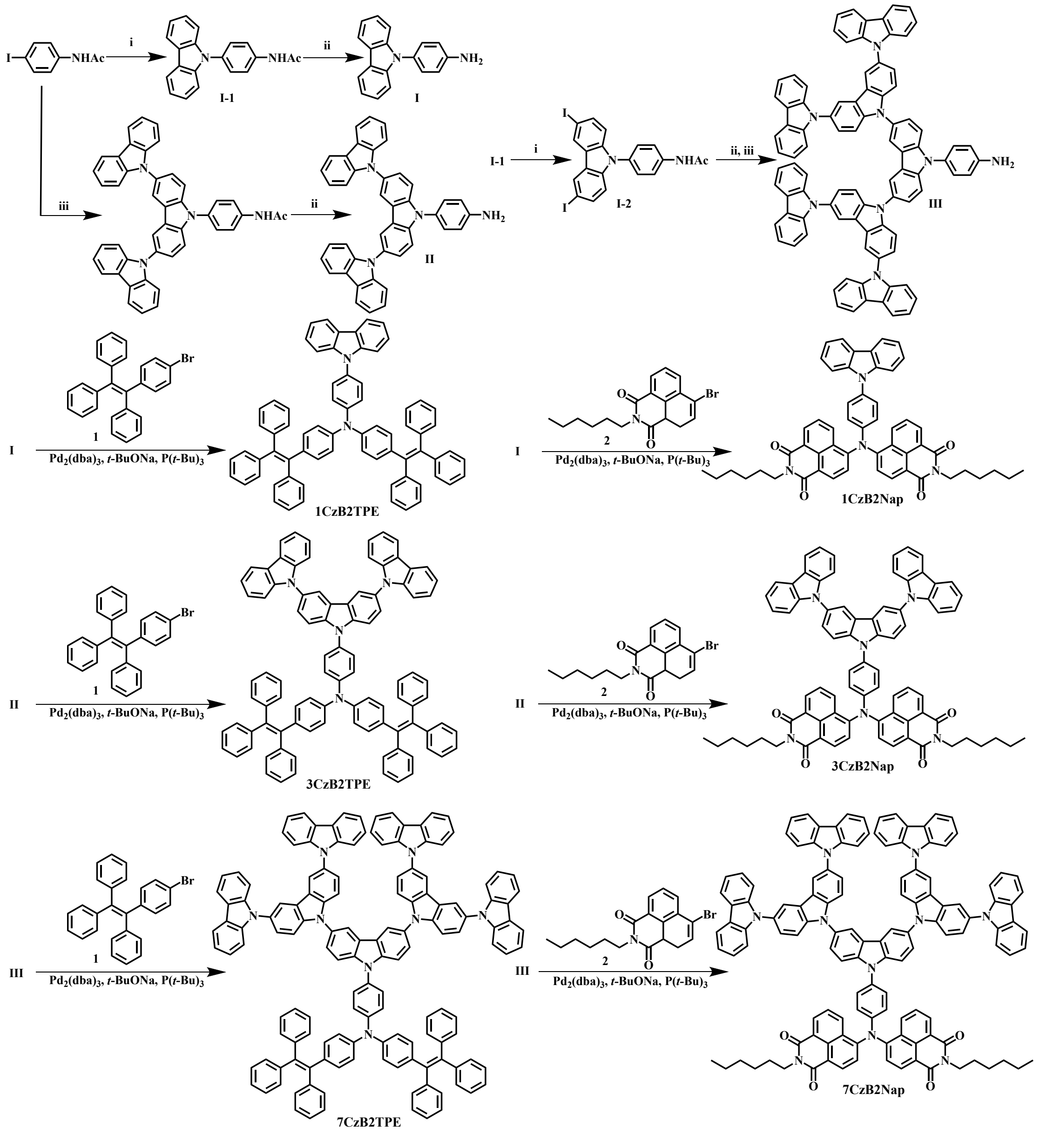

Scheme S1. Synthetic routes of carbazole derivatives **1CzB2TPE**, **3CzB2TPE**, **7CzB2TPE**, **1CzB2Nap**, **3CzB2Nap** and **7CzB2Nap**. Reagents and conditions: (i) carbazole, Cu_2O, DMAc, 24 h; (ii) H_2SO_4, H_2O, THF, MeOH, 2 h; (iii) carbazole dendron Cu_2O, DMAc, 24 h.

3. Figures S1-S6

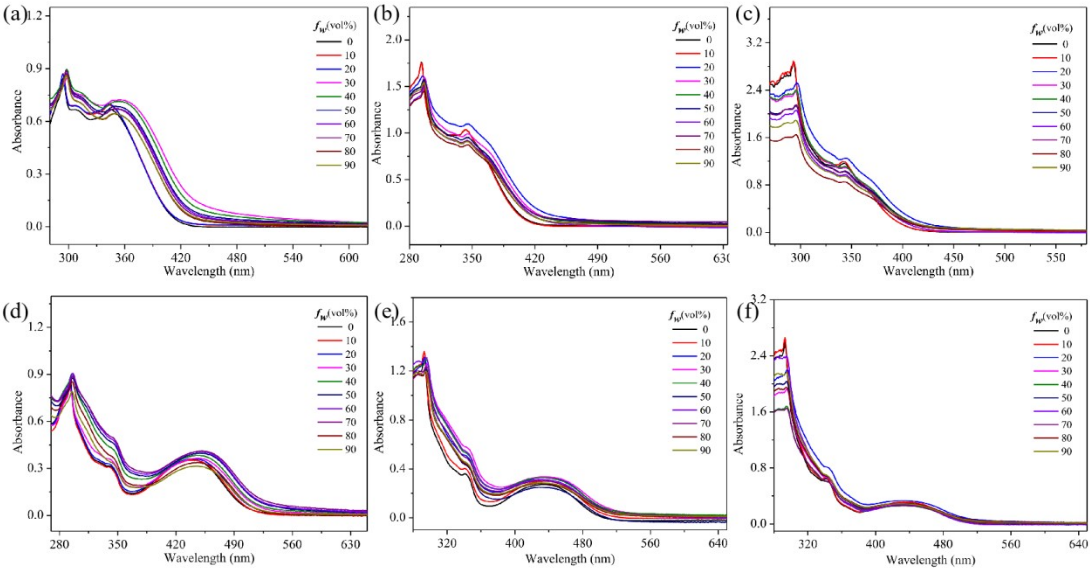

Figure S1. UV-Vis absorption spectra of compounds (2.0×10^{-5} mol L^{-1}) in DMF/water mixtures with different f_w values: (a) **1CzB2TPE**; (b) **3CzB2TPE**; (c) **7CzB2TPE**; (d) **1CzB2Nap**; (e) **3CzB2Nap**; (f) **7CzB2Nap**.

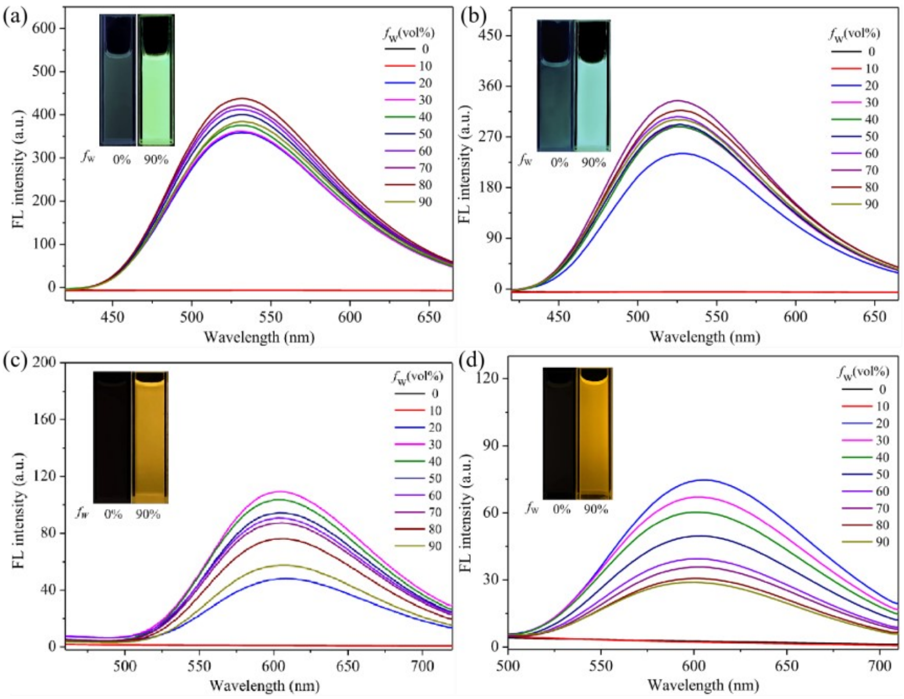

Figure S2. PL spectra of compounds (2.0×10^{-5} mol L^{-1}) in DMF/water mixtures with different f_w values. Excitation wavelength = 365 nm. The insets show the fluorescence images of compounds (2.0×10^{-5} mol L^{-1}) in pure DMF as well as 90% water content under 365 nm UV light: (a) **1CzB2TPE**; (b) **7CzB2TPE**; (c) **3CzB2Nap**; (d) **7CzB2Nap**.

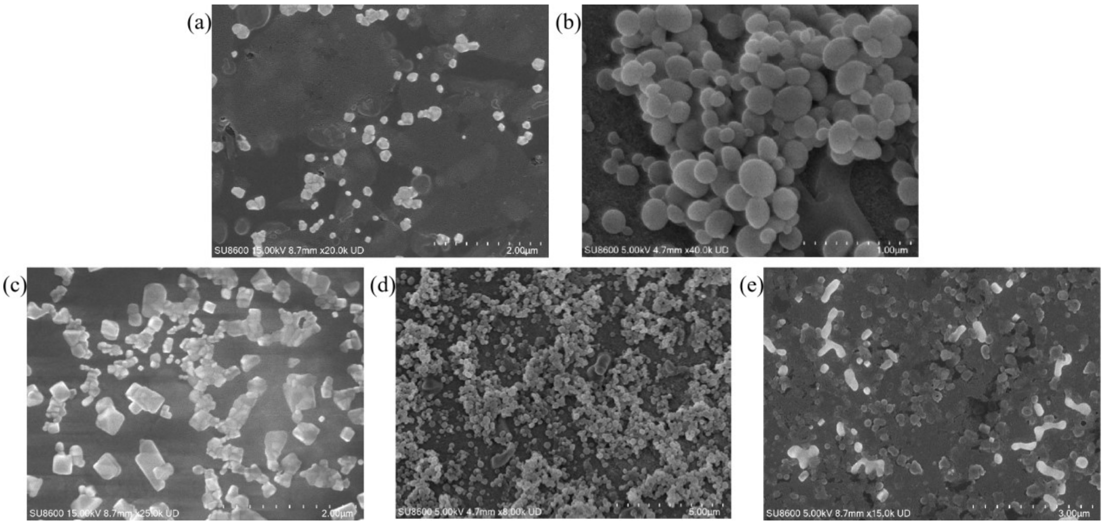

Figure S3. SEM images of compounds (2.0×10^{-5} mol L^{-1}) formed from DMF/water mixture (f_w = 90%): (a) **1CzB2TPE**; (b) **3CzB2TPE**; (c) **7CzB2TPE**; (d) **1CzB2Nap**; (e) **7CzB2Nap**.

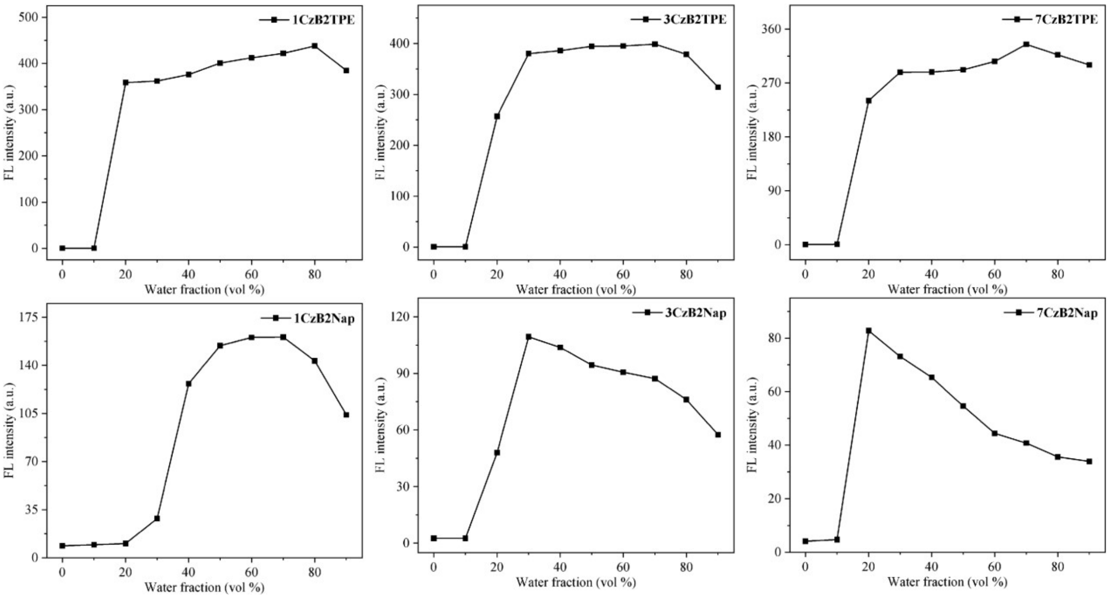

Figure S4. Plot of the relationship between maximum emission peak intensity and the f_W value of luminogen **1CzB2TPE**, **3CzB2TPE**, **7CzB2TPE**, **1CzB2Nap**, **3CzB2Nap** or **7CzB2Nap**.

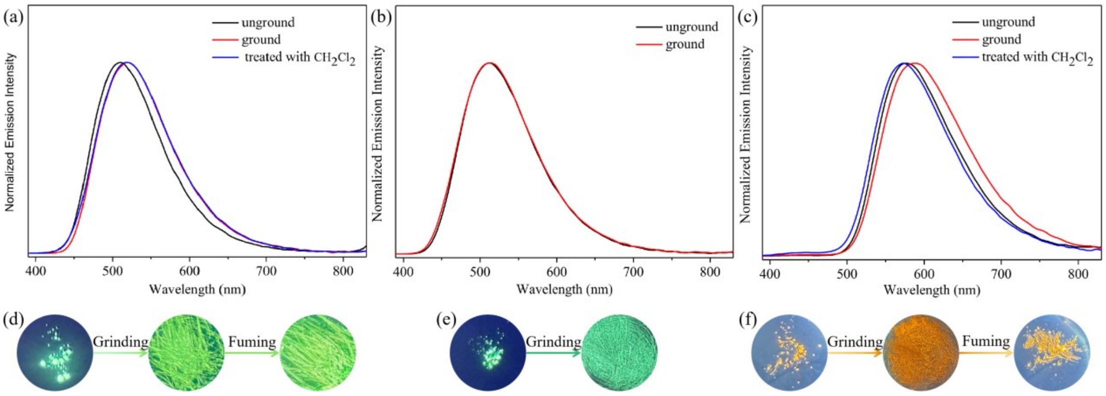

Figure S5. PL spectra of compounds in different solid states. Excitation wavelength = 365 nm: (a) **1CzB2TPE**; (b) **7CzB2TPE**; (c) **7CzB2Nap**. Photographic images of fluorogens in different solid states under 365 nm UV light: (d) **1CzB2TPE**; (e) **7CzB2TPE**; (f) **7CzB2Nap**.

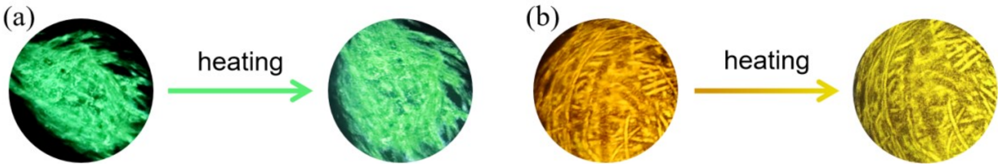

Figure S6. Photographic images of solids **3CzB2TPE** and **1CzB2Nap** before and after heating under 365 nm UV light: (a) **3CzB2TPE**; (b) **1CzB2Nap**.

4. Tables S1 and S2

Table S1. The maximum emission wavelength (λ_{max}) values of six reported compounds in various solid states.

Compound	**λ_{max} (before grinding)**	**λ_{max} (after grinding)**	**$\Delta\lambda$ (before and after grinding)**	**λ_{max} (fuming with CH_2Cl_2)**	**$\Delta\lambda$ (ground solid before and after fuming)**
1CzB2TPE	510 nm	519 nm	9 nm	518 nm	1 nm
3CzB2TPE	483 nm	517 nm	34 nm	517 nm	0
7CzB2TPE	512 nm	513 nm	1 nm	\	\
1CzB2Nap	563 nm	583 nm	20 nm	561 nm	22 nm
3CzB2Nap	581 nm	582 nm	1 nm	\	\
7CzB2Nap	576 nm	588 nm	12 nm	573 nm	15 nm

Table S2. The absolute fluorescence quantum yields (Φ_F) values and average fluorescence lifetimes of six reported compounds before and after grinding

Compound	Φ_F (before grinding)	Φ_F (after grinding)	Average fluorescence lifetime (<τ>, before grinding)	Average fluorescence lifetime (<τ>, after grinding)
1CzB2TPE	43%	21%	3.22 ns	2.70 ns
3CzB2TPE	37%	20%	2.49 ns	2.65 ns
7CzB2TPE	28%	17%	2.93 ns	2.67 ns
1CzB2Nap	30%	18%	3.68 ns	3.84 ns
3CzB2Nap	26%	16%	7.59 ns	8.00 ns
7CzB2Nap	17%	10%	8.61 ns	9.80 ns

5. Figures S7-S15

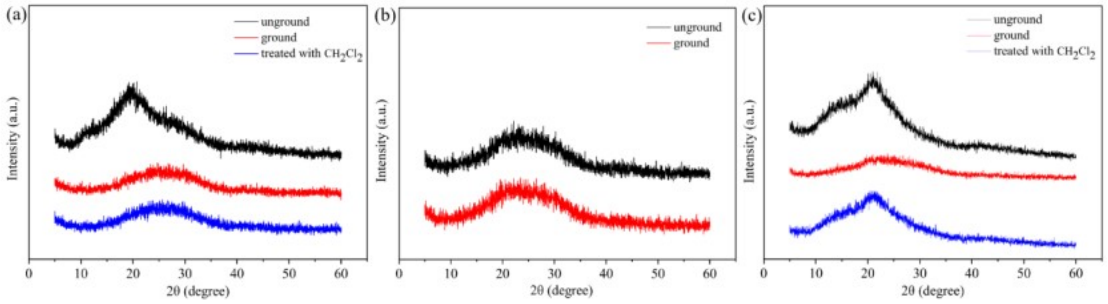

Figure S7. Powder XRD patterns of solids in various solid states. (a) **1CzB2TPE**; (b) **7CzB2TPE**; (c) **7CzB2Nap**.

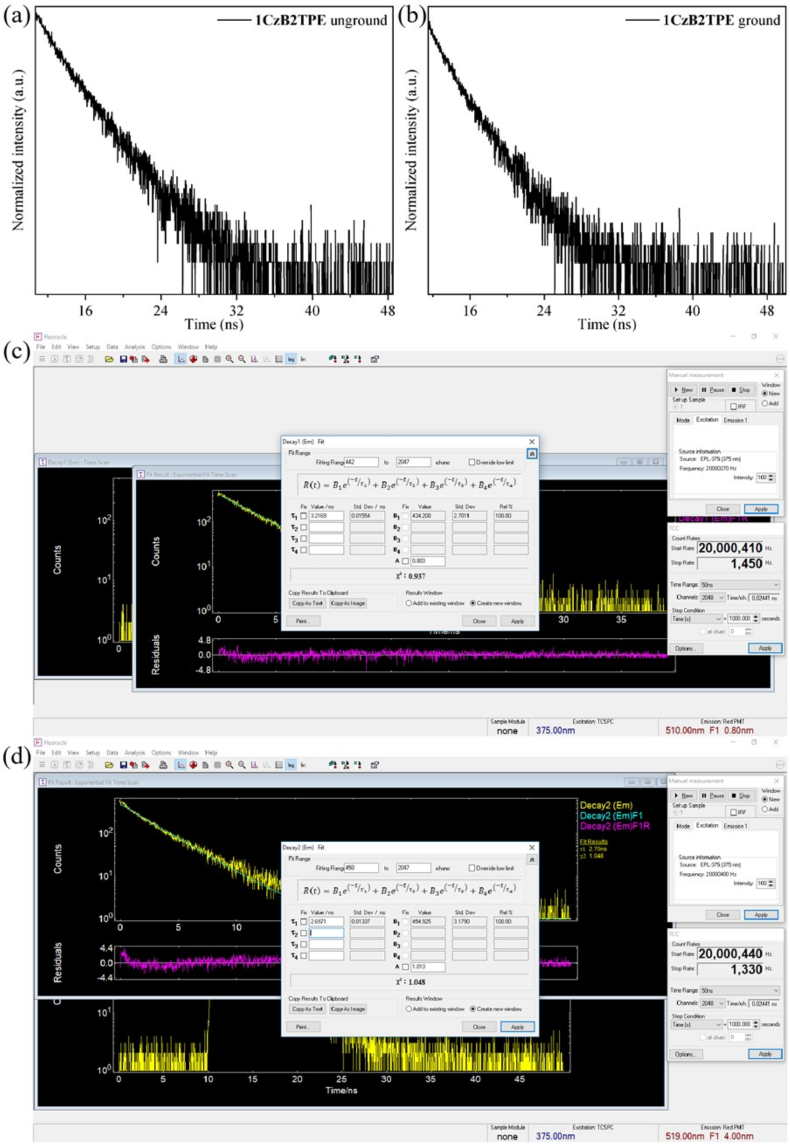

(c)

Decay1 (Em) Fit

Fit Range: Fitting Range 442 to 2047 chans ☐ Override low limit

$$R(t) = B_1e^{(-t/\tau_1)} + B_2e^{(-t/\tau_2)} + B_3e^{(-t/\tau_3)} + B_4e^{(-t/\tau_4)}$$

	Fix	Value / ns	Std. Dev / ns		Fix	Value	Std. Dev	Rel %
τ_1	☐	3.2169	0.01554	B_1		434.200	2.7011	100.00
τ_2	☐			B_2				
τ_3	☐			B_3				
τ_4	☐			B_4				
				A	☐	0.803		

χ^2 : 0.937

Results Window: ○ Add to existing window ● Create new window

Count Rates: Start Rate 20,000,410 Hz; Stop Rate 1,450 Hz

Sample Module none; Excitation TCSPC 375.00nm; Emission Red PMT 510.00nm F1 0.80nm

(d)

Decay2 (Em) Fit

Fit Range: Fitting Range 458 to 2047 chans ☐ Override low limit

$$R(t) = B_1e^{(-t/\tau_1)} + B_2e^{(-t/\tau_2)} + B_3e^{(-t/\tau_3)} + B_4e^{(-t/\tau_4)}$$

	Fix	Value / ns	Std. Dev / ns		Fix	Value	Std. Dev	Rel %
τ_1	☐	2.6971	0.01337	B_1		494.925	3.1790	100.00
τ_2	☐			B_2				
τ_3	☐			B_3				
τ_4	☐			B_4				
				A	☐	1.013		

χ^2 : 1.048

Results Window: ○ Add to existing window ● Create new window

Count Rates: Start Rate 20,000,440 Hz; Stop Rate 1,330 Hz

Sample Module none; Excitation TCSPC 375.00nm; Emission Red PMT 519.00nm F1 4.00nm

Figure S8. Decay curves of solid **1CzB2TPE** before (a) and after (b) grinding. Fitting data of solid **1CzB2TPE** before (c) and after (d) grinding. Excitation wavelength: 375 nm.

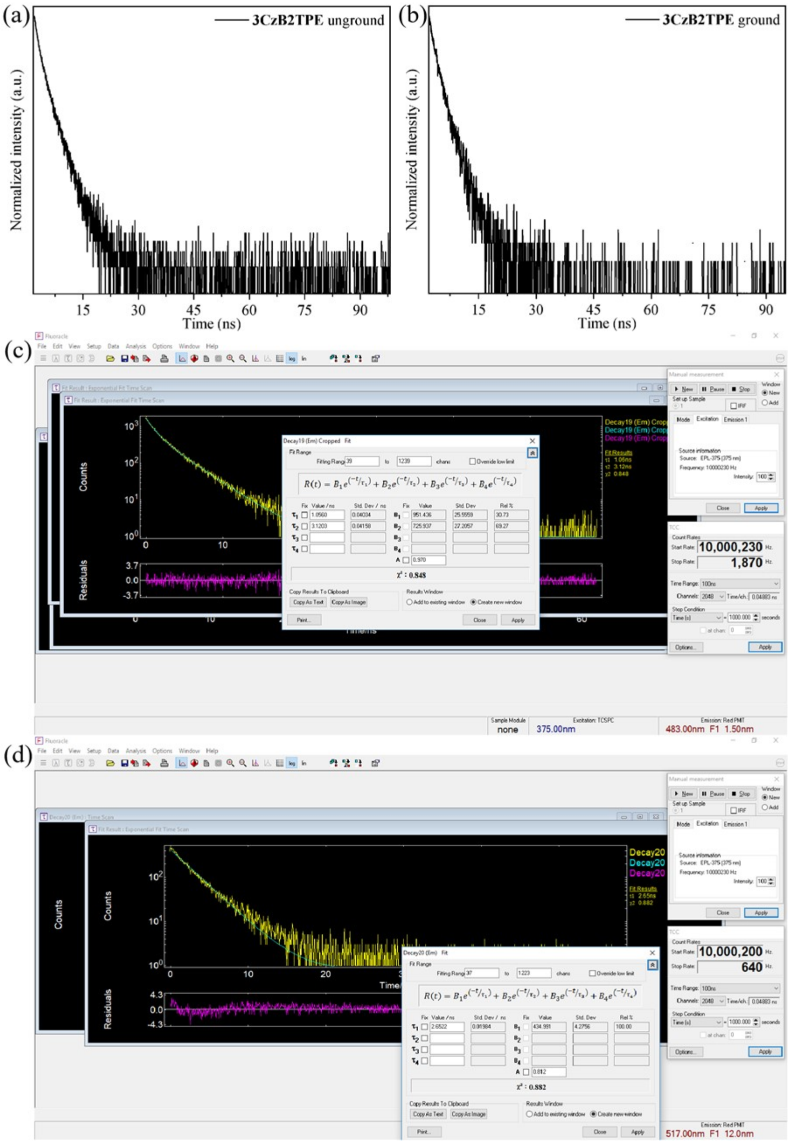

(c) Decay19 (Em) Cropped Fit

Fit Range: Fitting Range 39 to 1239 chans ☐ Override low limit

$R(t) = B_1e^{(-t/\tau_1)} + B_2e^{(-t/\tau_2)} + B_3e^{(-t/\tau_3)} + B_4e^{(-t/\tau_4)}$

	Fix	Value / ns	Std. Dev / ns		Fix	Value	Std. Dev	Rel %
τ_1	☐	1.0560	0.04034	B_1		951.436	25.5559	30.73
τ_2	☐	3.1203	0.04158	B_2		725.937	27.2057	69.27
τ_3	☐			B_3				
τ_4	☐			B_4				
				A	☐	0.970		

χ^2 : 0.848

Results Window: ○ Add to existing window ● Create new window

Fit Results: τ1 1.06ns τ2 3.12ns χ2 0.848

Start Rate: 10,000,230 Hz; Stop Rate: 1,870 Hz

Excitation: 375.00nm; Emission: 483.00nm F1 1.50nm

(d) Decay20 (Em) Fit

Fit Range: Fitting Range 37 to 1223 chans ☐ Override low limit

$R(t) = B_1e^{(-t/\tau_1)} + B_2e^{(-t/\tau_2)} + B_3e^{(-t/\tau_3)} + B_4e^{(-t/\tau_4)}$

	Fix	Value / ns	Std. Dev / ns		Fix	Value	Std. Dev	Rel %
τ_1	☐	2.6522	0.01984	B_1		434.991	4.2756	100.00
τ_2	☐			B_2				
τ_3	☐			B_3				
τ_4	☐			B_4				
				A	☐	0.812		

χ^2 : 0.882

Results Window: ○ Add to existing window ● Create new window

Fit Results: τ1 2.65ns χ2 0.882

Start Rate: 10,000,200 Hz; Stop Rate: 640 Hz

Emission: 517.00nm F1 12.0nm

Figure S9. Decay curves of solid **3CzB2TPE** before (a) and after (b) grinding. Fitting data of solid **3CzB2TPE** before (c) and after (d) grinding. Excitation wavelength: 375 nm.

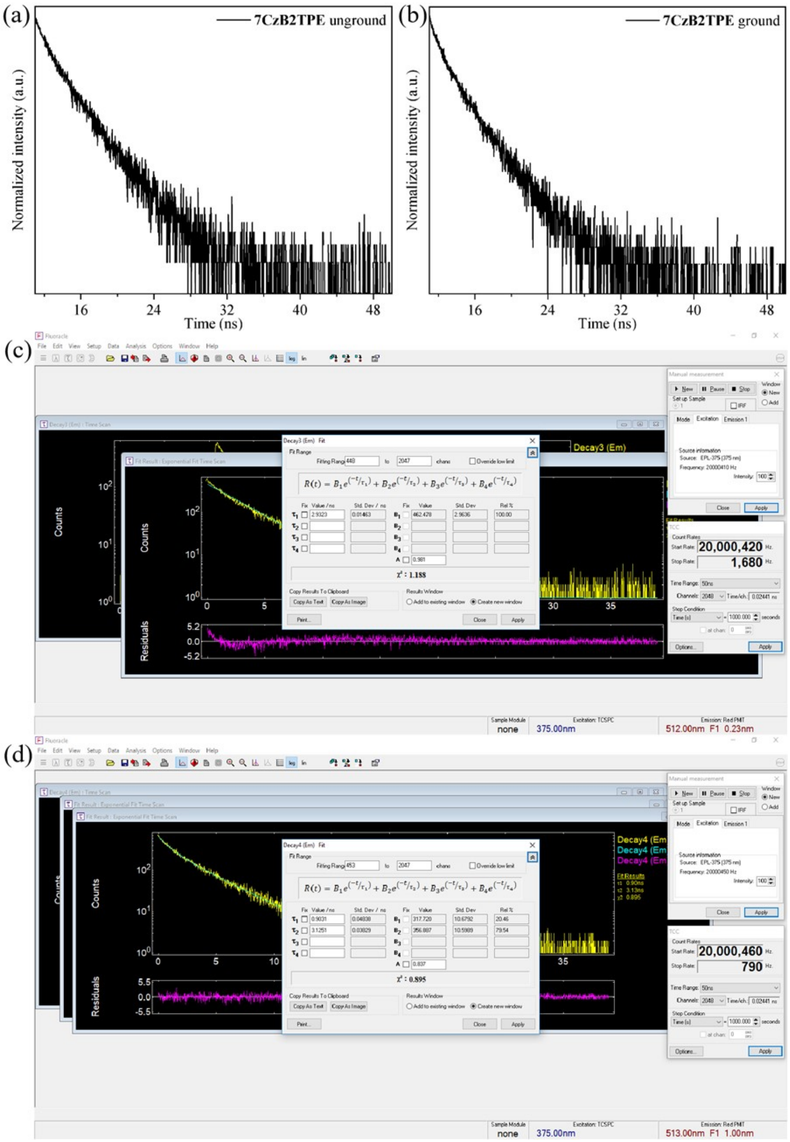

(c)

Decay3 (Em) Fit

Fitting Range 448 to 2047 chans ☐ Override low limit

$R(t) = B_1e^{(-t/\tau_1)} + B_2e^{(-t/\tau_2)} + B_3e^{(-t/\tau_3)} + B_4e^{(-t/\tau_4)}$

	Fix	Value / ns	Std. Dev / ns		Fix	Value	Std. Dev	Rel %
τ_1	☐	2.9323	0.01463	B_1	☐	462.478	2.9636	100.00
τ_2	☐			B_2	☐			
τ_3	☐			B_3	☐			
τ_4	☐			B_4	☐			
				A	☐	0.981		

χ^2 : 1.188

Results Window: ○ Add to existing window ● Create new window

Count Rates: Start Rate 20,000,420 Hz; Stop Rate 1,680 Hz

Sample Module none; Excitation 375.00nm; Emission 512.00nm F1 0.23nm

(d)

Decay4 (Em) Fit

Fitting Range 453 to 2047 chans ☐ Override low limit

$R(t) = B_1e^{(-t/\tau_1)} + B_2e^{(-t/\tau_2)} + B_3e^{(-t/\tau_3)} + B_4e^{(-t/\tau_4)}$

	Fix	Value / ns	Std. Dev / ns		Fix	Value	Std. Dev	Rel %
τ_1	☐	0.9031	0.04838	B_1	☐	317.720	10.6792	20.46
τ_2	☐	3.1251	0.03829	B_2	☐	356.887	10.5989	79.54
τ_3	☐			B_3	☐			
τ_4	☐			B_4	☐			
				A	☐	0.837		

χ^2 : 0.895

Results Window: ○ Add to existing window ● Create new window

Count Rates: Start Rate 20,000,460 Hz; Stop Rate 790 Hz

Sample Module none; Excitation 375.00nm; Emission 513.00nm F1 1.00nm

Figure S10. Decay curves of solid **7CzB2TPE** before (a) and after (b) grinding. Fitting data of solid **7CzB2TPE** before (c) and after (d) grinding. Excitation wavelength: 375 nm.

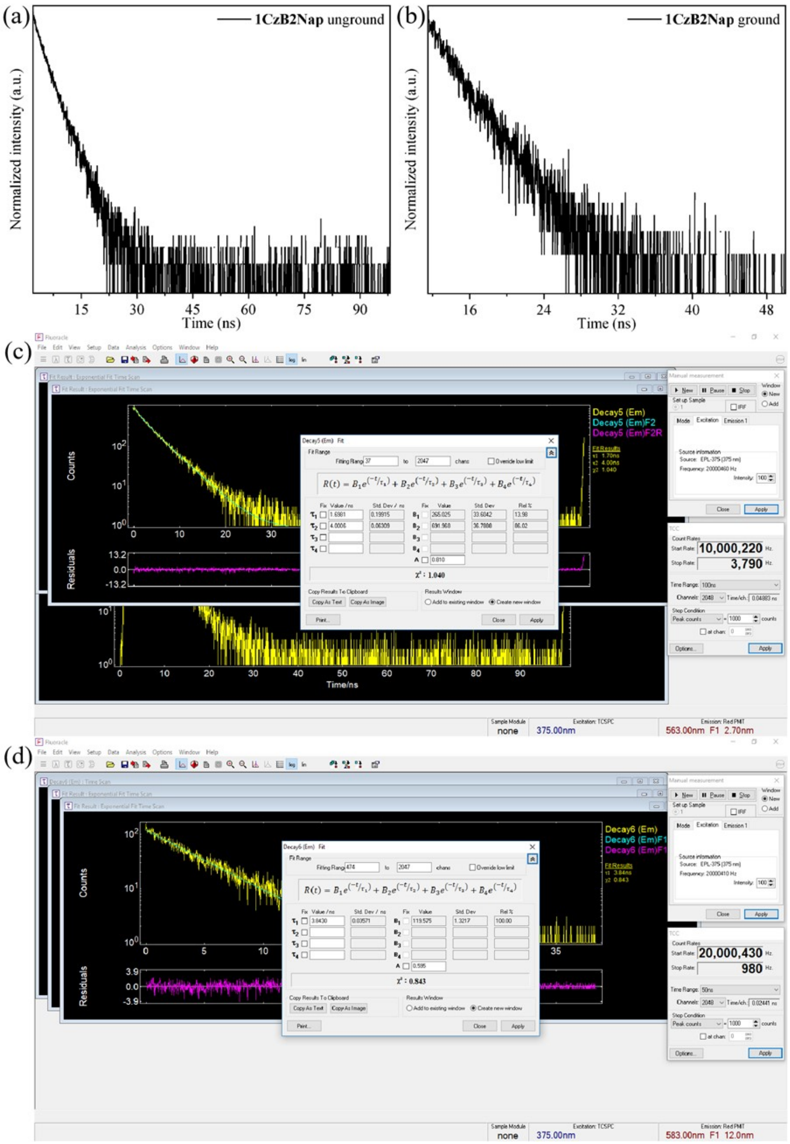

(c)

Decay5 (Em) Fit

Fit Range: Fitting Range 37 to 2047 chans ☐ Override low limit

$R(t) = B_1e^{(-t/\tau_1)} + B_2e^{(-t/\tau_2)} + B_3e^{(-t/\tau_3)} + B_4e^{(-t/\tau_4)}$

	Fix	Value / ns	Std. Dev / ns		Fix	Value	Std. Dev	Rel %
τ_1	☐	1.6981	0.19915	B_1	☐	265.025	33.6042	13.98
τ_2	☐	4.0006	0.06309	B_2	☐	691.968	36.7888	86.02
τ_3	☐			B_3	☐			
τ_4	☐			B_4	☐			
				A	☐	0.810		

χ^2 : 1.040

Copy Results To Clipboard

Results Window: ○ Add to existing window ● Create new window

Fit Results
τ1 1.70ns
τ2 4.00ns
χ2 1.040

Window: ● New ○ Add

☐ IRF

Source information
Source: EPL-375 (375 nm)
Frequency: 20000460 Hz
Intensity: 100

TCC
Count Rates
Start Rate: 10,000,220 Hz.
Stop Rate: 3,790 Hz.
Time Range: 100ns
Channels: 2048 Time/ch: 0.04883 ns
Stop Condition: Peak counts = 1000 counts
☐ at chan: 0

Sample Module: none
Excitation: TCSPC 375.00nm
Emission: Red PMT 563.00nm F1 2.70nm

(d)

Decay6 (Em) Fit

Fit Range: Fitting Range 474 to 2047 chans ☐ Override low limit

$R(t) = B_1e^{(-t/\tau_1)} + B_2e^{(-t/\tau_2)} + B_3e^{(-t/\tau_3)} + B_4e^{(-t/\tau_4)}$

	Fix	Value / ns	Std. Dev / ns		Fix	Value	Std. Dev	Rel %
τ_1	☐	3.8430	0.03571	B_1	☐	119.575	1.3217	100.00
τ_2	☐			B_2	☐			
τ_3	☐			B_3	☐			
τ_4	☐			B_4	☐			
				A	☐	0.595		

χ^2 : 0.843

Copy Results To Clipboard

Results Window: ○ Add to existing window ● Create new window

Fit Results
τ1 3.84ns
χ2 0.843

Window: ● New ○ Add

☐ IRF

Source information
Source: EPL-375 (375 nm)
Frequency: 20000410 Hz
Intensity: 100

TCC
Count Rates
Start Rate: 20,000,430 Hz.
Stop Rate: 980 Hz.
Time Range: 50ns
Channels: 2048 Time/ch: 0.02441 ns
Stop Condition: Peak counts = 1000 counts
☐ at chan: 0

Sample Module: none
Excitation: TCSPC 375.00nm
Emission: Red PMT 583.00nm F1 12.0nm

Figure S11. Decay curves of solid **1CzB2Nap** before (a) and after (b) grinding. Fitting data of solid **1CzB2Nap** before (c) and after (d) grinding. Excitation wavelength: 375 nm.

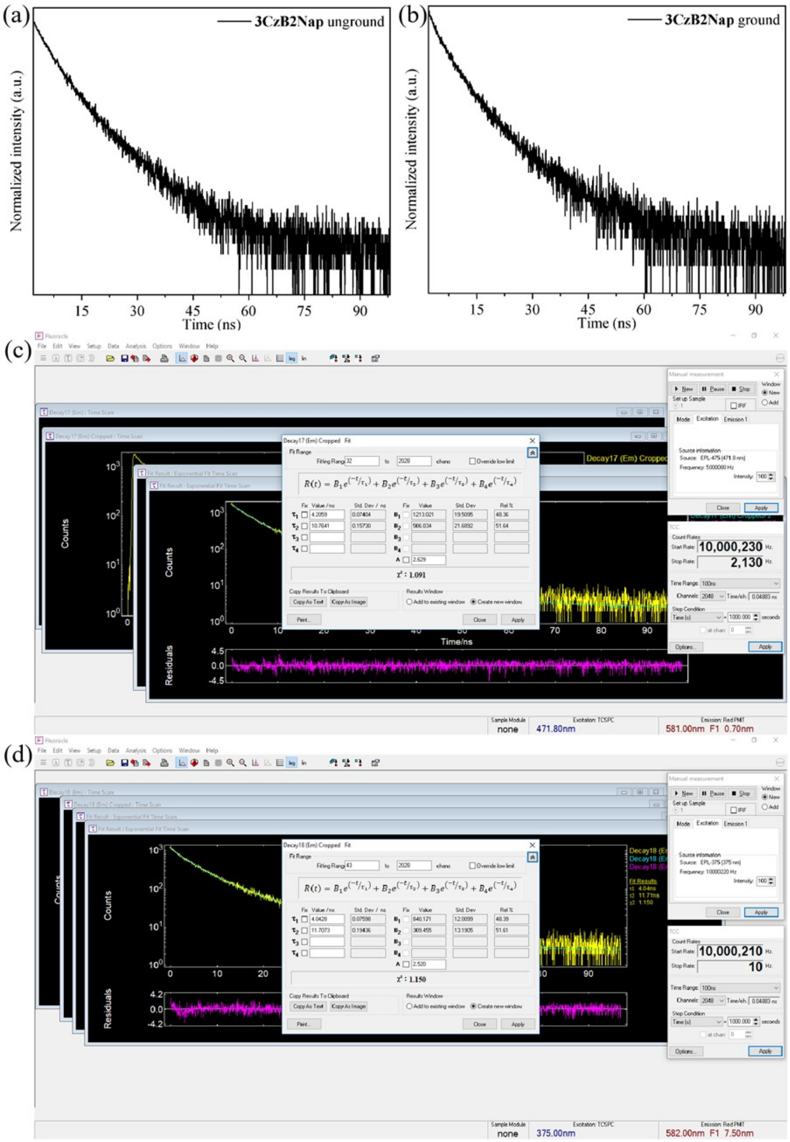

(c) Decay17 (Em) Cropped Fit

Fitting Range 32 to 2028 chans ☐ Override low limit

$$R(t) = B_1e^{(-t/\tau_1)} + B_2e^{(-t/\tau_2)} + B_3e^{(-t/\tau_3)} + B_4e^{(-t/\tau_4)}$$

	Fix	Value / ns	Std. Dev / ns		Fix	Value	Std. Dev	Rel %
τ_1	☐	4.2059	0.07404	B_1	☐	1213.021	19.5095	48.36
τ_2	☐	10.7641	0.15730	B_2	☐	506.034	21.6892	51.64
τ_3	☐			B_3	☐			
τ_4	☐			B_4	☐			
				A	☐	2.629		

χ^2 : 1.091

Results Window: ○ Add to existing window ● Create new window

Sample Module none; 471.80nm; 581.00nm F1 0.70nm

(d) Decay18 (Em) Cropped Fit

Fitting Range 43 to 2028 chans ☐ Override low limit

$$R(t) = B_1e^{(-t/\tau_1)} + B_2e^{(-t/\tau_2)} + B_3e^{(-t/\tau_3)} + B_4e^{(-t/\tau_4)}$$

	Fix	Value / ns	Std. Dev / ns		Fix	Value	Std. Dev	Rel %
τ_1	☐	4.0428	0.07598	B_1	☐	840.171	12.0099	48.39
τ_2	☐	11.7073	0.19436	B_2	☐	309.455	13.1905	51.61
τ_3	☐			B_3	☐			
τ_4	☐			B_4	☐			
				A	☐	2.520		

χ^2 : 1.150

Results Window: ○ Add to existing window ● Create new window

Sample Module none; 375.00nm; 582.00nm F1 7.50nm

Figure S12. Decay curves of solid **3CzB2Nap** before (a) and after (b) grinding. Fitting data of solid **3CzB2Nap** before (c) and after (d) grinding. Excitation wavelength: 375 nm.

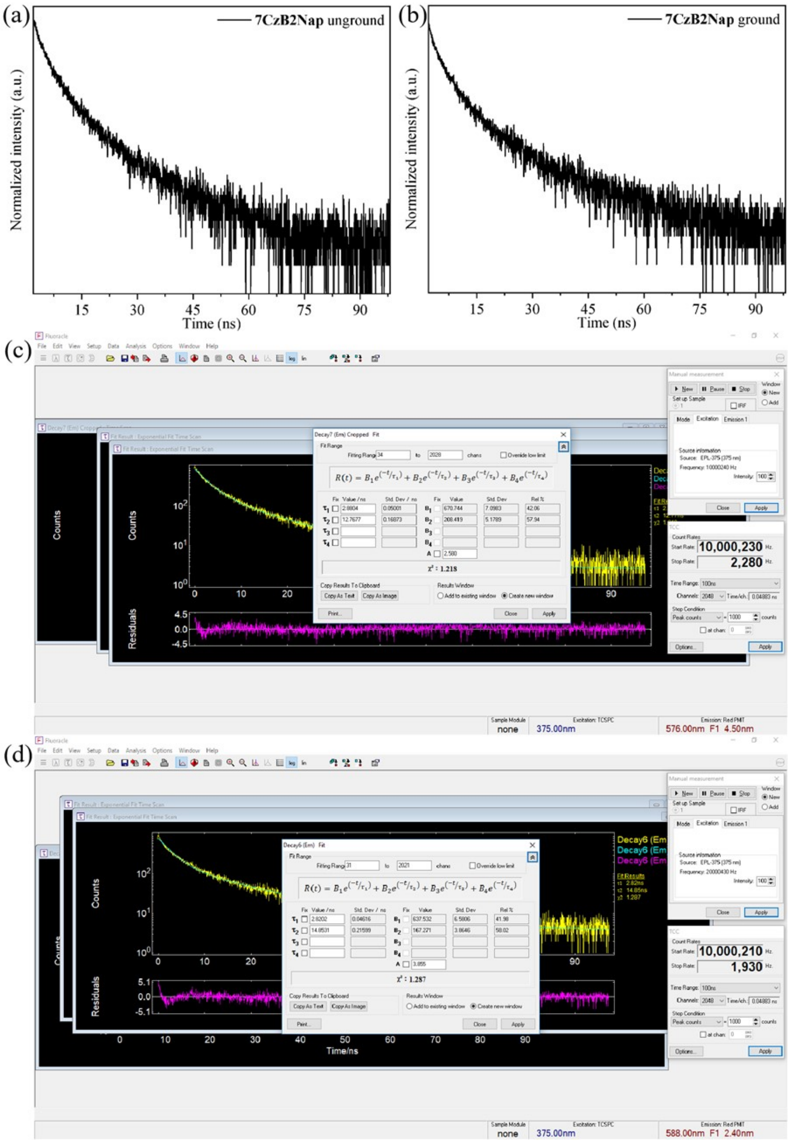

(c)

Decay7 (Em) Cropped Fit

Fit Range: Fitting Range 34 to 2028 chans ☐ Override low limit

$$R(t) = B_1e^{(-t/\tau_1)} + B_2e^{(-t/\tau_2)} + B_3e^{(-t/\tau_3)} + B_4e^{(-t/\tau_4)}$$

	Fix	Value / ns	Std. Dev / ns		Fix	Value	Std. Dev	Rel %
τ_1	☐	2.8804	0.05001	B_1		670.744	7.0983	42.06
τ_2	☐	12.7677	0.16873	B_2		208.419	5.1789	57.94
τ_3	☐			B_3				
τ_4	☐			B_4				
				A	☐	2.580		

χ^2 : 1.218

Results Window: ○ Add to existing window ● Create new window

Manual measurement: Window ● New ○ Add; Set up Sample 1; ☐ IRF; Mode / Excitation / Emission 1

Source information: Source: EPL-375 (375 nm); Frequency: 10000240 Hz; Intensity: 100

TCC Count Rates: Start Rate: 10,000,230 Hz; Stop Rate: 2,280 Hz

Time Range: 100ns; Channels: 2048; Time/ch.: 0.04883 ns

Stop Condition: Peak counts = 1000 counts; ☐ at chan: 0

Sample Module: none; Excitation: TCSPC 375.00nm; Emission: Red PMT 576.00nm F1 4.50nm

(d)

Decay6 (Em) Fit

Fit Range: Fitting Range 31 to 2021 chans ☐ Override low limit

$$R(t) = B_1e^{(-t/\tau_1)} + B_2e^{(-t/\tau_2)} + B_3e^{(-t/\tau_3)} + B_4e^{(-t/\tau_4)}$$

	Fix	Value / ns	Std. Dev / ns		Fix	Value	Std. Dev	Rel %
τ_1	☐	2.8202	0.04616	B_1		637.532	6.5806	41.98
τ_2	☐	14.8531	0.21599	B_2		167.221	3.8646	58.02
τ_3	☐			B_3				
τ_4	☐			B_4				
				A	☐	3.855		

χ^2 : 1.287

Results Window: ○ Add to existing window ● Create new window

Fit Results: τ1 2.82ns; τ2 14.85ns; χ2 1.287

Source information: Source: EPL-375 (375 nm); Frequency: 20000430 Hz; Intensity: 100

TCC Count Rates: Start Rate: 10,000,210 Hz; Stop Rate: 1,930 Hz

Time Range: 100ns; Channels: 2048; Time/ch.: 0.04883 ns

Stop Condition: Peak counts = 1000 counts; ☐ at chan: 0

Sample Module: none; Excitation: TCSPC 375.00nm; Emission: Red PMT 588.00nm F1 2.40nm

Figure S13. Decay curves of solid **7CzB2Nap** before (a) and after (b) grinding. Fitting data of solid **7CzB2Nap** before (c) and after (d) grinding. Excitation wavelength: 375 nm.

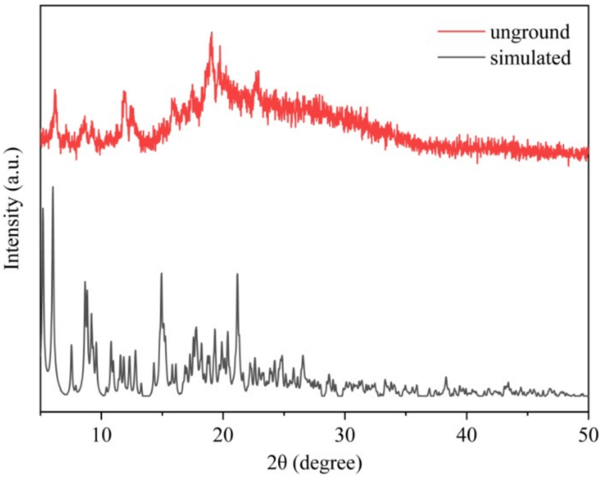

Figure S14. Simulated powder XRD pattern of **3CzB2TPE** crystal and powder XRD pattern of unground solid **3CzB2TPE**.

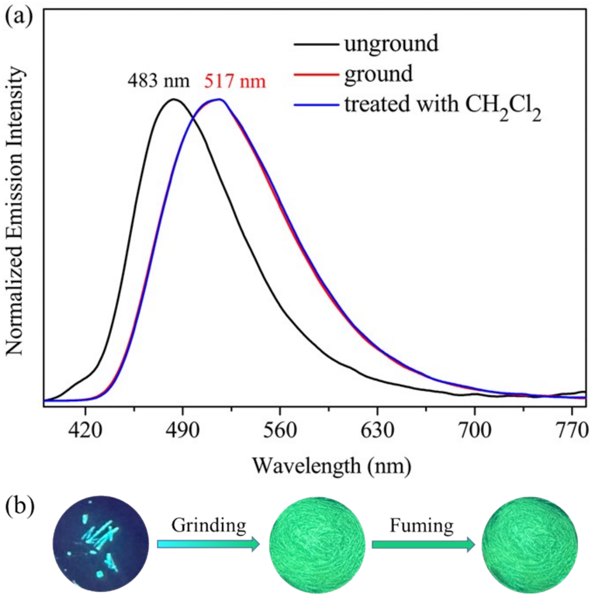

Figure S15. (a) Normalized PL spectra of **3CzB2TPE** crystals before grinding, after grinding, and after treatment with dichloromethane vapor. Excitation wavelength: 365 nm. (b) Photographic photographs of **3CzB2TPE** crystals before grinding, after grinding, and after treatment with dichloromethane vapor under 365 nm UV light.

6. NMR spectra and HRMS spectra of carbazole derivatives

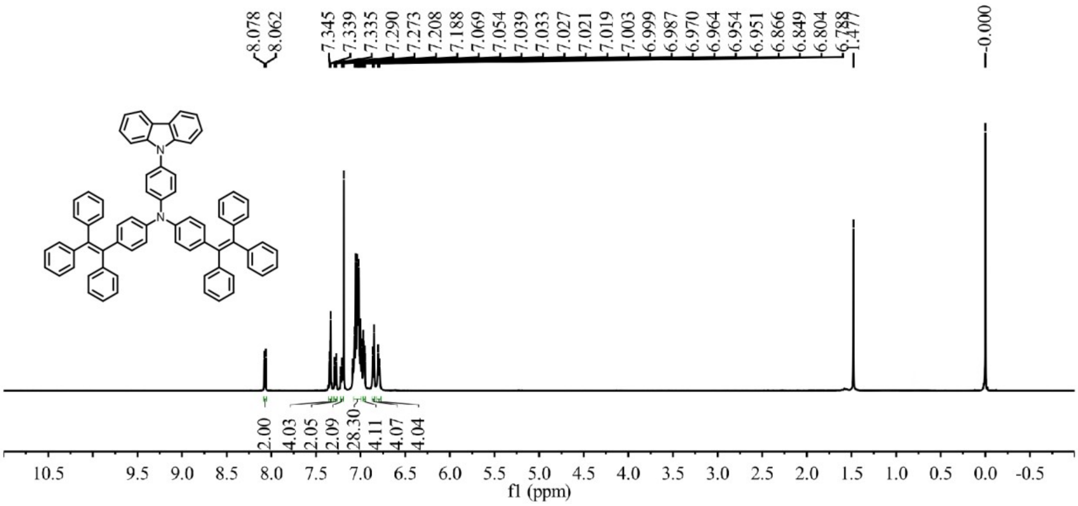

^{1}H NMR spectrum of carbazole derivative **1CzB2TPE**

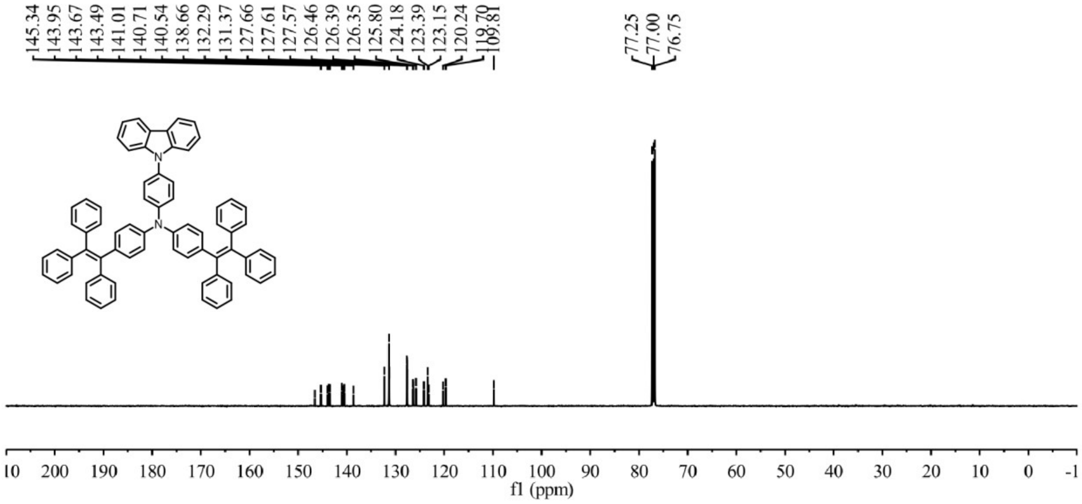

^{13}C NMR spectrum of carbazole derivative **1CzB2TPE**

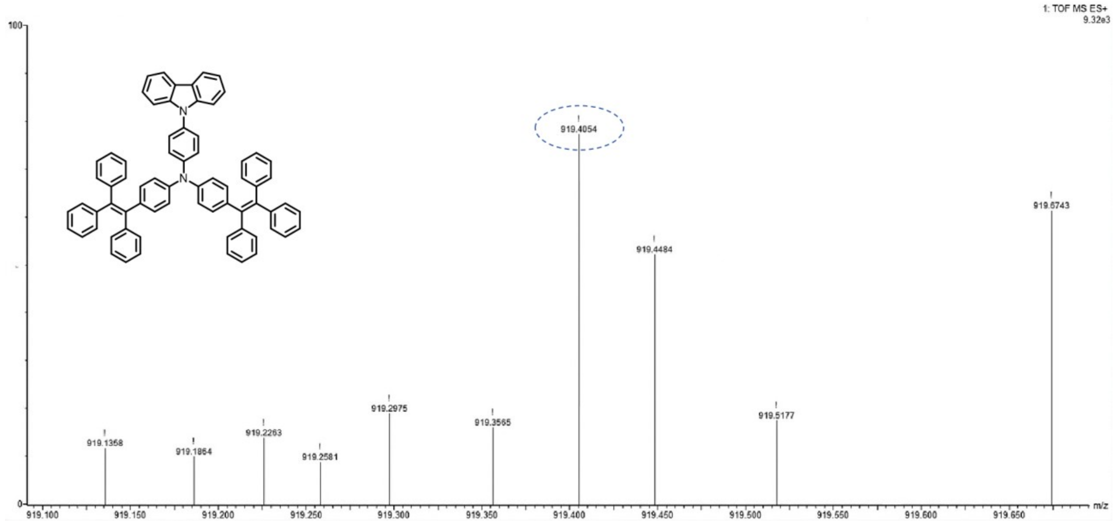

HRMS spectrum of carbazole derivative **1CzB2TPE**

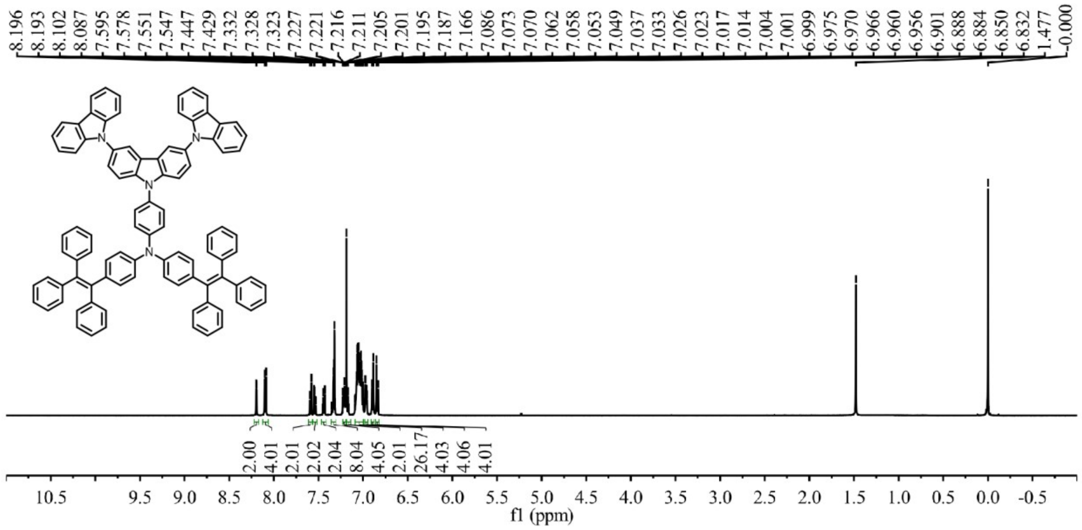

^{1}H NMR spectrum of carbazole derivative **3CzB2TPE**

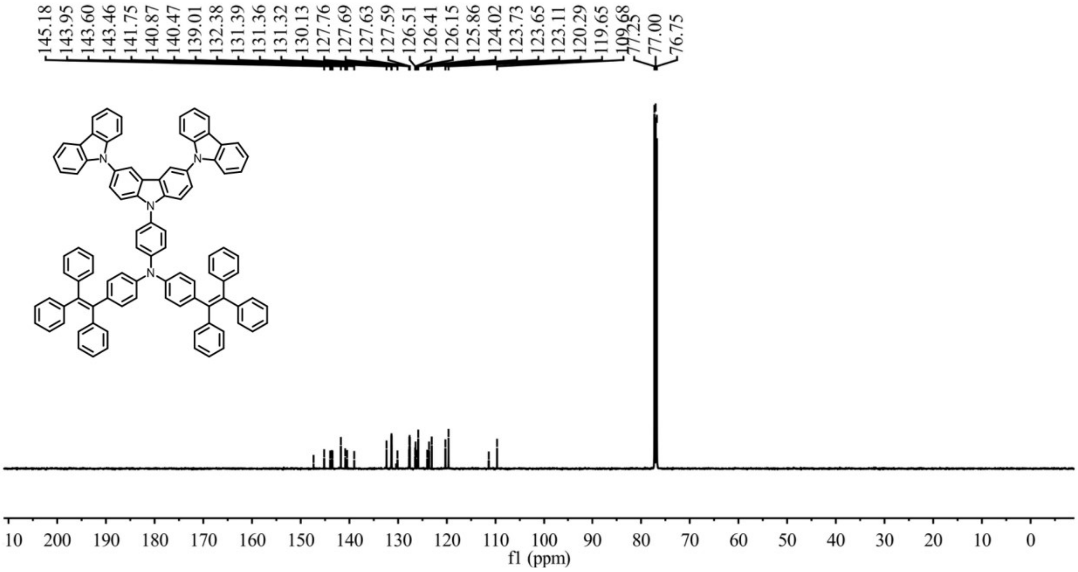

^{13}C NMR spectrum of carbazole derivative **3CzB2TPE**

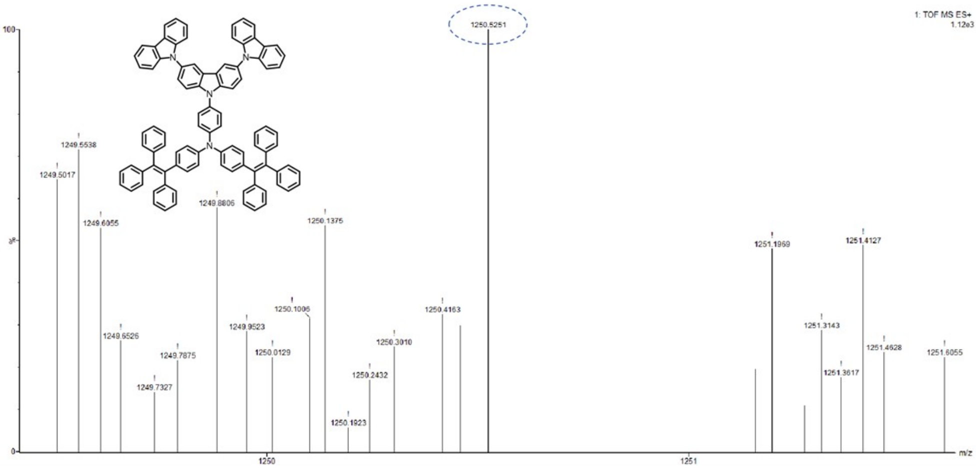

HRMS spectrum of carbazole derivative **3CzB2TPE**

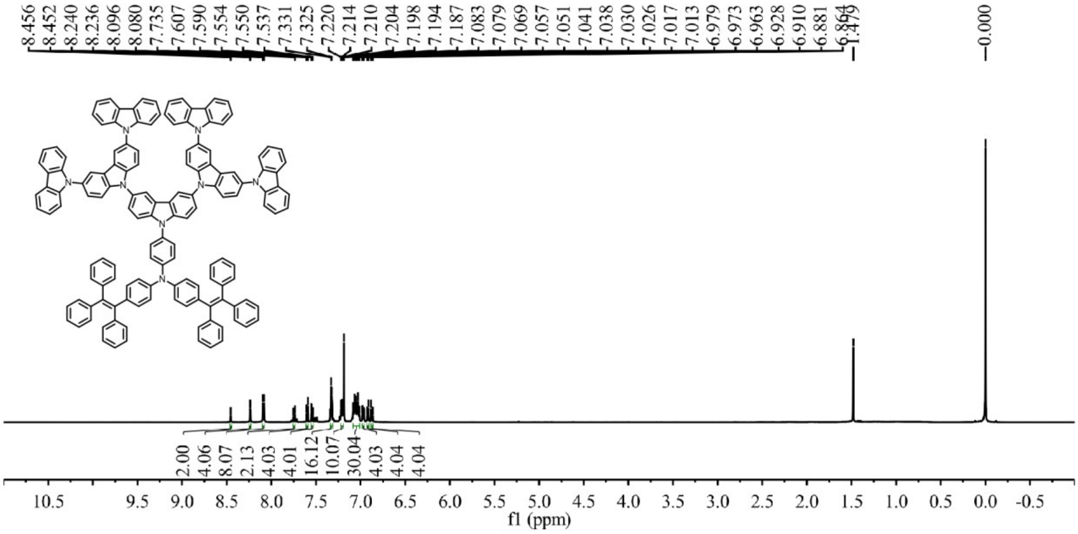

^{1}H NMR spectrum of carbazole derivative **7CzB2TPE**

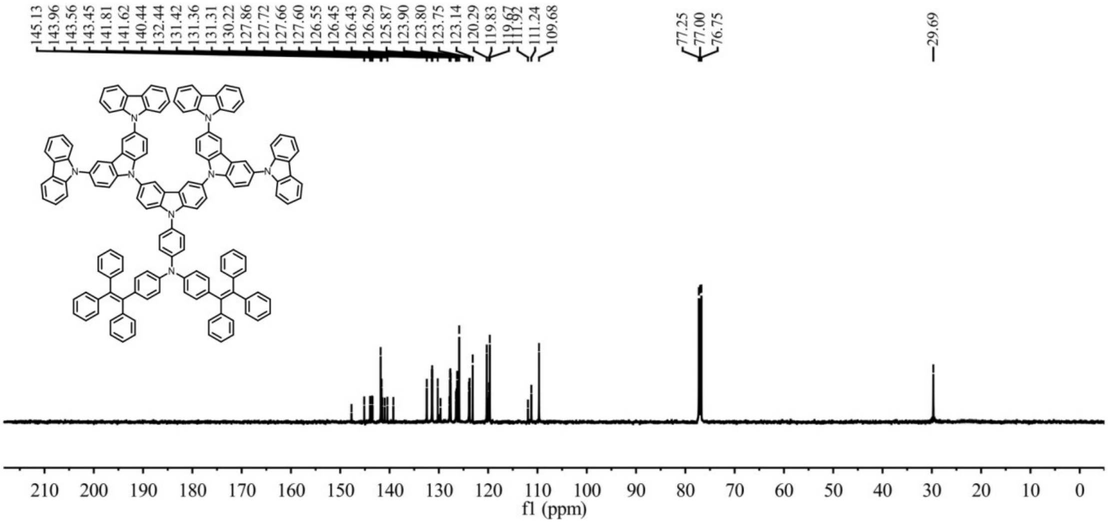

^{13}C NMR spectrum of carbazole derivative **7CzB2TPE**

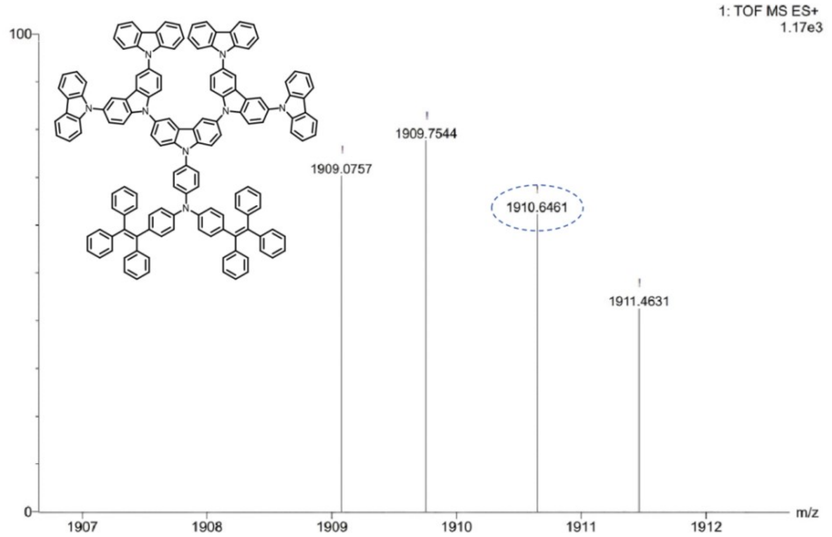

HRMS spectrum of carbazole derivative **7CzB2TPE**

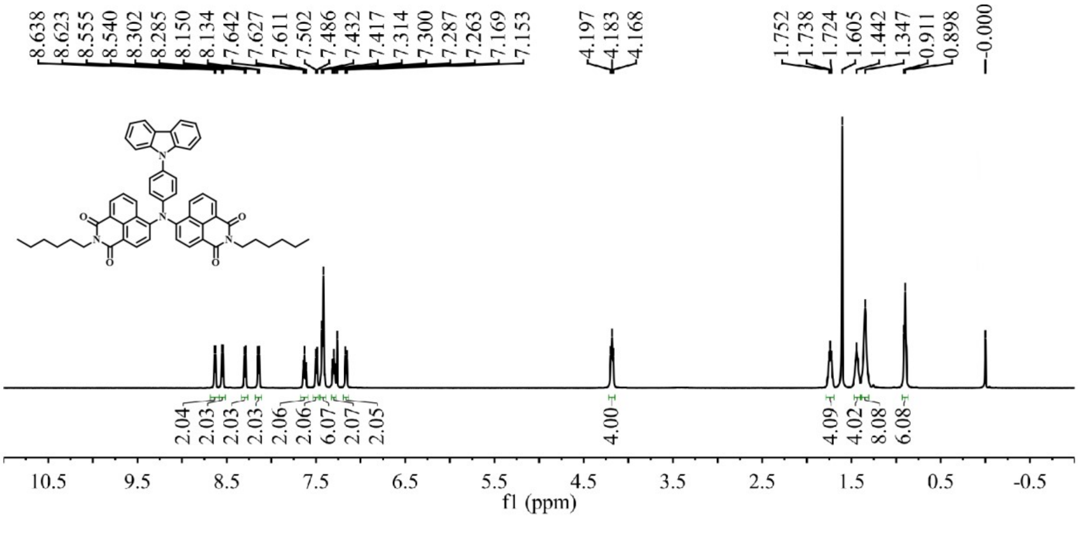

^{1}H NMR spectrum of carbazole derivative **1CzB2Nap**

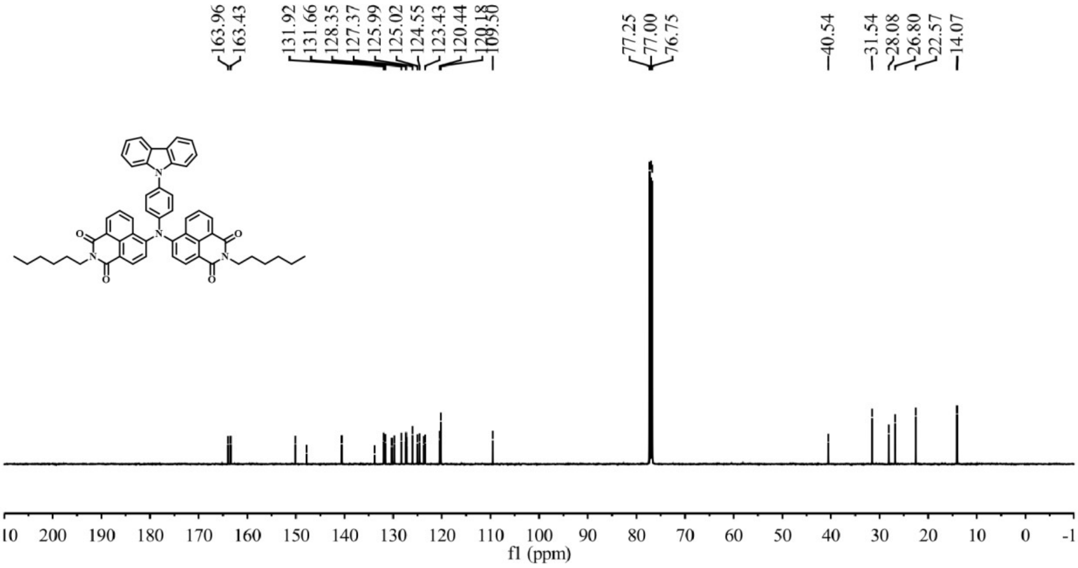

^{13}C NMR spectrum of carbazole derivative **1CzB2Nap**

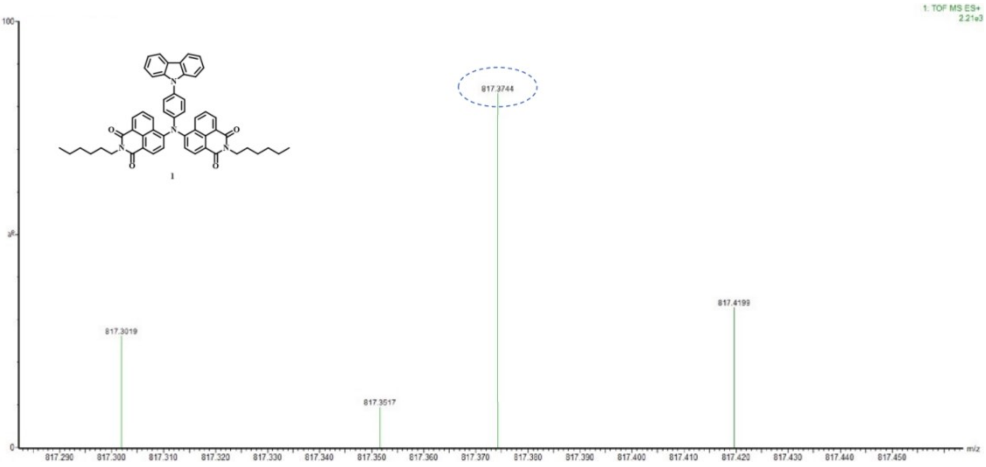

HRMS spectrum of carbazole derivative **1CzB2Nap**

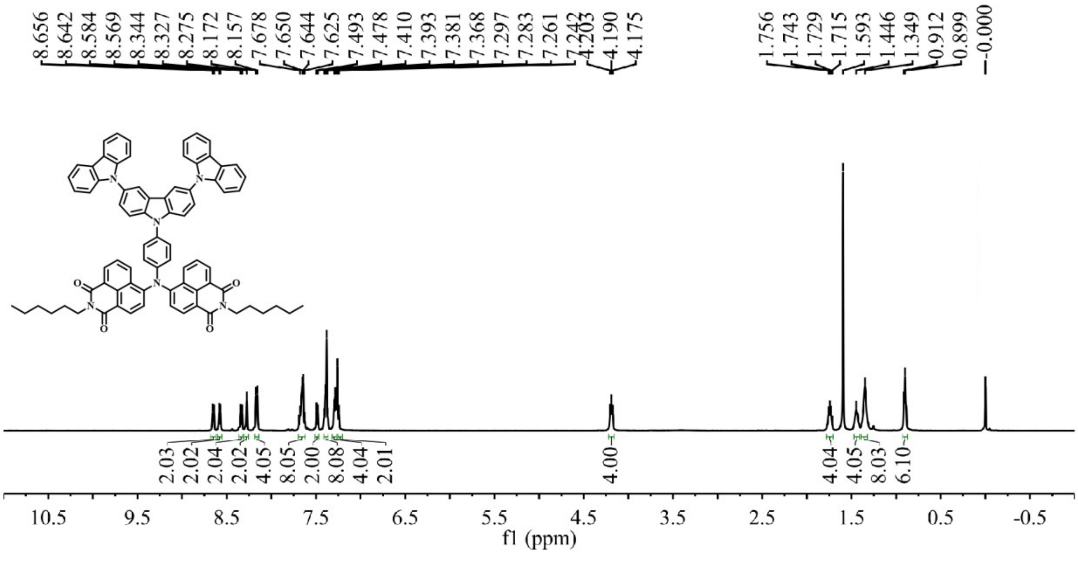

^{1}H NMR spectrum of carbazole derivative **3CzB2Nap**

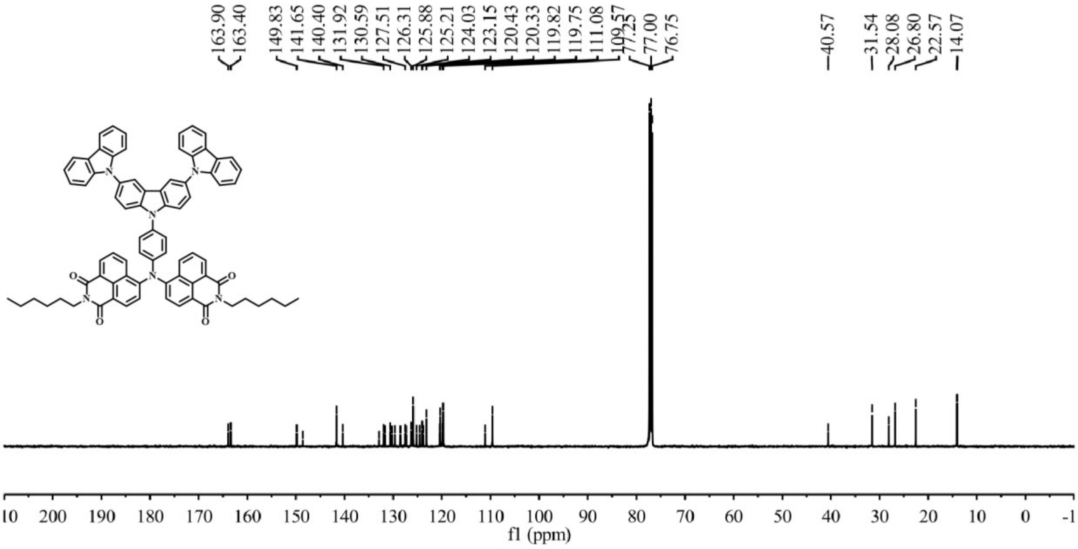

^{13}C NMR spectrum of carbazole derivative **3CzB2Nap**

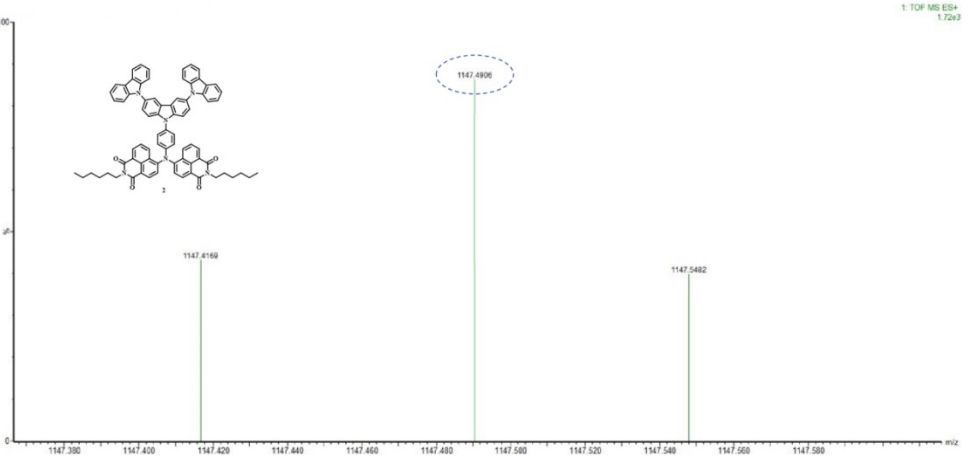

HRMS spectrum of carbazole derivative **3CzB2Nap**

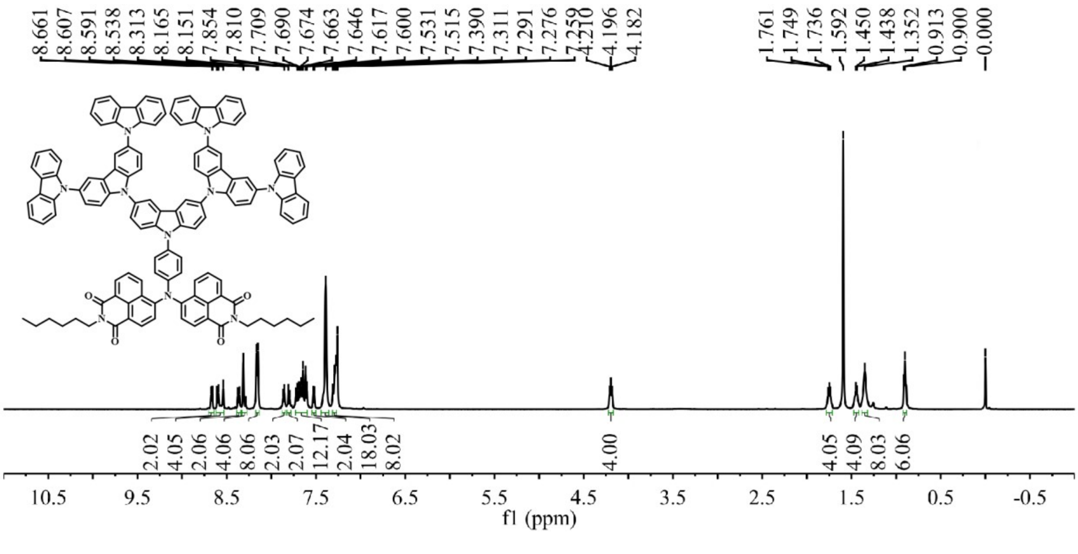

^{1}H NMR spectrum of carbazole derivative **7CzB2Nap**

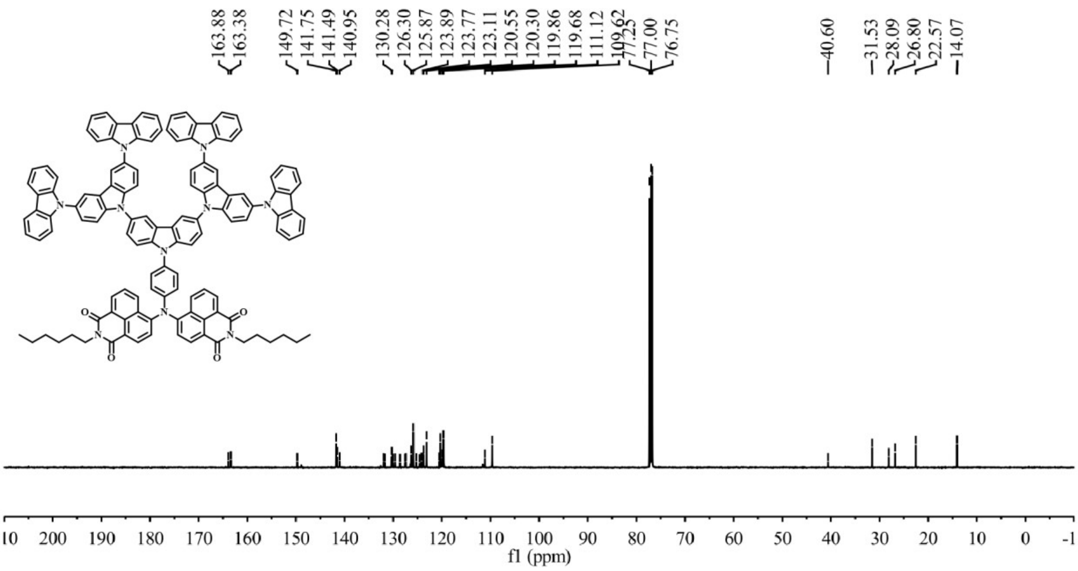

^{13}C NMR spectrum of carbazole derivative **7CzB2Nap**

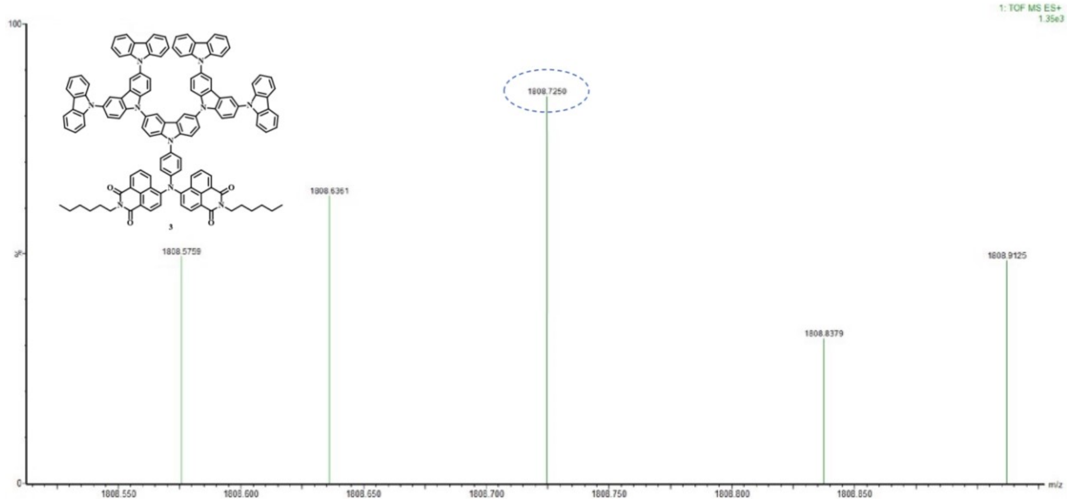

HRMS spectrum of carbazole derivative **7CzB2Nap**

7. References

(1) A. Kimoto, J.-S. Cho, M. Higuchi and K. Yamamoto, Synthesis of asymmetrically arranged dendrimers with a carbazole dendron and a phenylazomethine dendron, *Macromolecules*, 2004, **37**, 5531-5537.

(2) F. Zhao, Z. Chen, C. Fan, G. Liu and S. Pu, Aggregation-induced emission (AIE)-active highly emissive novel carbazole-based dyes with various solid-state fluorescence and reversible mechanofluorochromism characteristics, *Dyes Pigments*, 2019, **164**, 390-397.

(3) P. J. Stephens, F. J. Devlin, C. F. Chabalowski and M. J. Frisch, Ab initio calculation of vibrational absorption and circular dichroism spectra using density functional force fields, *J. Phys. Chem.*, 1994, **98**, 11623-11627.

(4) S. Grimme, S. Ehrlich and L. Goerigk, Effect of the damping function in dispersion corrected density functional theory, *J. Comput. Chem.*, 2011, **32**, 456-1465.

(5) W. J. Hehre, R. Ditchfield and J. A. Pople, Self-consistent molecular orbital methods. XII. further extensions of Gaussian-type basis sets for use in molecular orbital studies of organic molecules, *J. Chem. Phys.*, 1972, **56**, 2257-2261.

(6) T. Clark, J. Chandrasekhar, G. W. Spitznagel and P. V. R. Schleyer, Stabilization of methyl anions by first-row substituents. The superiority of diffuse function-augmented basis sets for anion calculations, *J. Comput. Chem.*, 1983, **4**, 294-301.

(7) S. S. Zade, N. Zamoshchik and M. Bendikov, From short conjugated oligomers to conjugated polymers. Lessons from studies on long conjugated oligomers, *Acc. Chem. Res.*, 2011, **44**, 14-24.

(8) T. Lu and F. Chen, Multiwfn: A multifunctional wavefunction analyzer, *J. Comput. Chem.*, 2012, **33**, 580-592.

(9) W. Humphrey, A. Dalke and K. Schulten, VMD: visual molecular dynamics, *J. Mol. Graph.*, 1996, **14**, 33-38.